Waste Management 84 (2019) 102–111

Contents lists available at ScienceDirect

Waste Management

journal homepage: www.elsevier.com/locate/wasman

Gas generation measurement and evaluation during mechanical processing and thermal treatment of spent Li-ion batteries

Fabian Diaz [a,*], Yufengnan Wang [a], Reiner Weyhe [b], Bernd Friedrich [a,*]

[a] Institute of Process Metallurgy and Metal Recycling IME, RWTH Aachen University, Intzestraße 3, 52056 Aachen, Germany
[b] ACCUREC Recycling GmbH, Bataverstr. 21, 47809 Krefeld, Germany

ARTICLE INFO

Article history:
Received 19 June 2018
Revised 13 November 2018
Accepted 16 November 2018

Keywords:
Li-ion batteries
Off-gas
Recycling
Thermal runaway
Quantitative analysis
Toxicity
Pyrolysis
Combustion
Mechanical treatment

ABSTRACT

Recycling of Li-ion batteries (LIBs) is becoming an urgent issue. However, the chemical composition and the hazard of off-gas produced during the recycling process still remain unclarified due to the complicated reactions during thermal runaway (TR). In order to meet the legislative requirements to carry out an environmentally friendly recycling, this manuscript aims to undertake quantitative analysis and toxicity evaluation of the off-gas produced in mechanical treatment and thermal treatment of LIBs. The measurements were carried out by online Fourier transform infrared spectroscopy (FTIR) and ion chromatograph (IC). The volume of total off-gas was calculated and its toxicity was evaluated by USA's Protective Action Criteria. The influences of treatment method, state-of-charge (SOC), atmosphere, and type of cathode were investigated.

1. Introduction

A battery is a device which can convert its inside chemical energy into outside electric energy (Linden and Reddy, 2002). Among all sorts of batteries in the market, lithium ion batteries (LIBs) in consumer electronics and electric vehicles (EV) are rapidly growing because of their high energy density, extended cycle-lifetime, and constant voltage output (Pillot, 2017b), resulting in boosting raw material demand and legislation required collection of spent LIBs (Zeng et al., 2014).

Looking at the future prospective of main LIB users, the market research and consulting firm, Avicenne energy, made assumptions that the portable devices will increase at a rate of 6% per year in volume from 2015 to 2025 (Pillot, 2013, 2017a), industrial and stationary demands will increase at a 16% average growth rate per year. The total hybrid electric vehicles (HEVs) market will achieve 4.8 million (M) units with 35% LIB in 2020 and around 7 M units with 90% LIB in 2025; this without including micro hybrid vehicles. It is quite difficult to forecast the full EV market. Assuming that on average an EV will need 25 kWh battery pack, it will achieve 0.6 M units in 2020 worldwide except for China and 1 M units in 2025, while China alone is expected to have 1 M EVs in 2020 and 1.5 M in 2025 (Pillot, 2017b, 2013). The cycle life time of a battery can be reached around 800–1500 charge cycles depending on the type of applications and individual habits. For example, the batteries would be replaced for a Battery Electric Vehicle (BEV) at 25% loss of the capacity, which can be around the warranty period or 8–10 years of a normal lifetime (Amarakoon et al., 2013; Bloom et al., 2001). LIB in consumer applications can also be dispose because of the change of modern technologies against out-of-date technologies, even before batteries reach a technical end-of-life (EOL). According to studies of the U.S. Environmental Protection Agency, 90% of all mobile devices in a given model year have been sent for their EOL management in less than five years (U.S. environmental protection agency, 2011). Although the spent LIBs are approaching their EOL, little residual power still remains (Doerffel and Sharkh, 2006). In general, there are many attempts to develop an efficient recycling process based on mechanical and thermal pretreatments (Georgi-Maschler et al., 2012; Wang and Friedrich, 2015). However, unlike other batteries, LIBs often explode during the recycling process due to radical oxidation when lithium metal produced from battery overcharge sustains a mechanical shock from exposure to the air. Such kinds of uncontrollable exothermic reactions is often called thermal runaway

* Corresponding authors.
E-mail addresses: fdiaz@ime-aachen.de (F. Diaz), bfriedrich@ime-aachen.de (B. Friedrich).

https://doi.org/10.1016/j.wasman.2018.11.029
0956-053X/

(TR) (Chen et al., 2006; Tobishima and Yamaki, 1999; Wang et al., 2012).

In a conventional LIBs recycling process, cells are commonly heated and shredded, which ultimately promote violent reactions and explosion during the handling process. Therefore, it is of great importance to analyze the compositions of the off-gases and clarify their hazards. Although lots of efforts have been made to study TR and its mechanisms, the gas emission of LIBs has been studied only to a limited extent. Therefore, the main focus of this study is firstly to understand the emissions recorded during pre-treatments (mechanical and thermal) and their expected toxicity, which was evaluated using the USA's Protective Action Criteria. The influences of treatment method, state-of-charge (SOC), atmosphere, and type of cathode are also investigated.

2. Basics on thermal runaway reactions and reported emission gases from LIBs

It is stated that TR could normally take place in case of abuse of the batteries like heating, short-circuit, overcharge, nail penetration, crushing. In literature, some observations have been reported like the influence of cathode material in the TR e.g. Lithium Manganese oxide (LMO) is safer than Lithium Cobalt oxide (LCO) (Tobishima and Yamaki, 1999); high risk of explosion during overheating, overcharge and short-circuit as a result of the increased internal heat and pressure (Chen et al., 2006); Ohsaki et al. studied overcharge reaction by heating the overcharged anode and cathode separately. Their results showed that the thermal runaway reaction during overcharge was caused by the violent reaction between the overcharged anode (deposited lithium) and the electrolyte solvent at high temperature which was the result of the rapid exothermic reaction of the delithiated cathode and the electrolyte (Ohsaki et al., 2005). It is reported that some techniques can be used to avoid explosion. For instance, discharging the batteries before the recycling process reduces the risks for the following treatments (Li et al., 2012, 2011; Sun and Qiu, 2011). There are approaches for the complete discharging of modules or batteries in a bath of a conductive liquid solution (e.g. sodium chloride, calcium carbonate, sulphuric acid, hydrochloric acid or nitric acid) or with the help of external resistances (Zeng et al., 2014; ELIBAMA, 2014). However, it is time consuming and hardly achieves full discharge for every cell.

The TR follows a mechanism of chain reactions, during which the reaction of the battery component materials occurs one after another (Feng et al., 2017). Although there are some differences among TR caused by different abuse conditions of different kinds of LIBs, the main reaction mechanism could be summarized in Fig. 1.

The initial decomposition of thin passivating Solid-Electrolyte Interphase (SEI) layer on the anode is regarded as the first step that occurs during the TR. The SEI layer is mainly consisted of stable (such as LiF, Li_2CO_3), and metastable components (such as polymers, $ROCO_2Li$, $(CH_2OCO_2Li)_2$ and ROLi). Some degradation reactions applied to the SEI are presented in Eqs. (1) and (2) (Chen et al., 2006; Feng et al., 2017; Spotnitz and Franklin, 2003; Wang et al., 2012).

$$(CH_2OCO_2Li)_2 \rightarrow Li_2CO_3 + C_2H_4 + CO_2 + 1/2O_2 \quad (1)$$

$$2Li + (CH_2OCO_2Li)_2 \rightarrow 2Li_2CO_3 + C_2H_4 \quad (2)$$

Once the SEI decomposes at high temperature, the intercalated lithium in the graphite anode has the chance to contact the electrolyte. Within ~120 °C–250 °C, the SEI decomposition and

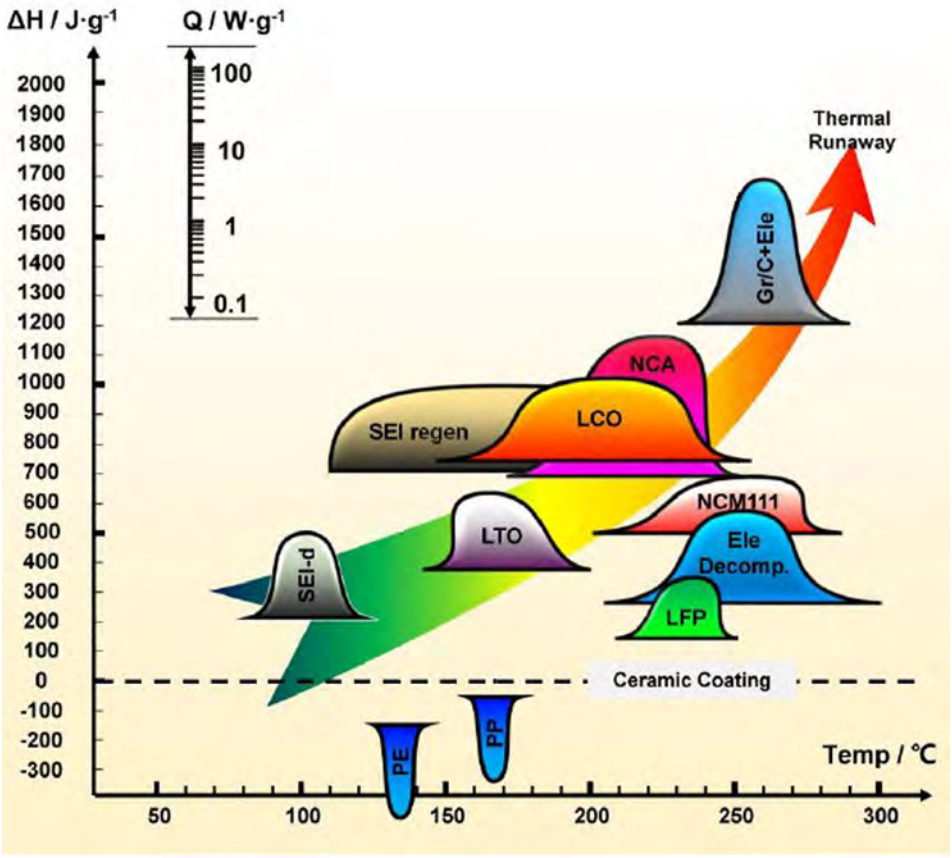

Fig. 1. Illustration of LIB thermal runaway mechanism (Feng et al., 2017).

regeneration occur simultaneously. When the structure of the SEI collapses, graphite anode decomposes with electrolyte. Some degradation reactions of the electrolyte solvent in contact with lithium are presented in Eqs. (3) and (4) (Feng et al., 2017).

$$2Li + C_3H_4O_3\ (EC) \rightarrow Li_2CO_3 + C_2H_4 \quad (3)$$

$$2Li + C_4H_6O_3\ (PC) \rightarrow Li_2CO_3 + C_3H_6 \quad (4)$$

$$2Li + C_3H_6O_3\ (DMC) \rightarrow Li_2CO_3 + C_2H_6 \quad (5)$$

Cathode decomposes when temperature reaches the onset temperature of their decomposition points. Some reactions occurring at the cathode are presented from Eqs. (6)-(9) (Chen et al., 2006; Feng et al., 2017; Spotnitz and Franklin, 2003; Tobishima and Yamaki, 1999; Wang et al., 2012).

$$Li_{0.5}CoO_2 \rightarrow 1/2LiCoO_2 + 1/6Co_3O_4 + 1/6O_2 \quad (6)$$

$$Li_{(1-x)}NiO_2 \rightarrow (1-2\,x)LiNiO_2 + xLiNi_2O_4\ (x \leq 0.5) \quad (7)$$

$$Li_{(1-x)}NiO_2 \rightarrow [Li_{(1-x)}Ni_{(2x-1)/3}]\,[Ni_{(4-2x)/3}]O_{(8-4x)/3} + (2x\text{-}1)/3O_2\ (x > 0.5) \quad (8)$$

$$Li_{(1-x)}NiO_2 \rightarrow (2\text{-}x)Li_{(1-x)/(2-x)}Ni_{1/(2-x)}O + x/2O_2 \quad (9)$$

Although lack of validation, Röder et al. (2013) proposed a possible mechanism of the $LiFePO_4$ (LFP) decomposition as for the delithiated Li_0FePO_4 (see Eq. (10)).

$$2Li_0FePO_4 \rightarrow Fe_2P_2O_7 + 1/2O_2 \quad (10)$$

The solvent also experience oxidation reactions when it is in contact with oxygen during e.g. a combustion process. Some reactions are presented from Eqs. (11)–(13).

$$5/2O_2 + C_3H_4O_3\ (EC) \rightarrow 3CO_2 + 2H_2O \quad (11)$$

$$4O_2 + C_4H_6O_3\ (PC) \rightarrow 4CO_2 + 3H_2O \quad (12)$$

$$3O_2 + C_3H_6O_3\ (DMC) \rightarrow 3CO_2 + 3H_2O \quad (13)$$

The electrolyte itself also decomposes at elevated temperature and produces many types of gas species. Some electrolyte degradation reactions documented previously are presented from Eqs. (14)–(21) (Chen et al., 2006; Feng et al., 2017; Kawamura et al., 2002; Spotnitz and Franklin, 2003; Tobishima and Yamaki, 1999; Wang et al., 2012).

$$LiPF_6 \rightleftharpoons LiF + PF_5 \quad (14)$$

$$LiPF_6 + H_2O \rightleftharpoons LiF + HF + POF_3 \quad (15)$$

$$C_2H_5OCOOC_2H_5 + PF_5 \rightarrow C_2H_5OCOOPF_4HF + C_2H_4 \quad (16)$$

$$C_2H_5OCOOC_2H_5 + PF_5 \rightarrow C_2H_5OCOOPF_4 + C_2H_5F \quad (17)$$

$$C_2H_5OCOOPF_4 \rightarrow HF + C_2H_4 + CO_2 + POF_3 \quad (18)$$

$$C_2H_5OCOOPF_4 \rightarrow C_2H_5F + CO_2 + POF_3 \quad (19)$$

$$C_2H_5OCOOPF_4 + HF \rightarrow PF_4OH + CO_2 + C_2H_5F \quad (20)$$

$$C_2H_5OH + C_2H_4 \rightarrow C_2H_5OC_2H_5 \quad (21)$$

In addition to the reactions listed above, the Polyethylene/Polypropylene (PE/PP) based separator will shrink and melt, when the temperature reaches their melting points, 135 °C and 165 °C, respectively. The separator melting is an endothermic process, so it would slow down the increasing rate of temperature.

Other reactions such as Polyvinylidene fluoride (PVDF) binder decomposition (Ortner and Hensler, 1995), lithium (either metallic or intercalated) reacting with a fluorinated binder (Eq. (22)), and Lithium metal reactions have little influence on the TR behavior (see Eq. (22)) (Feng et al., 2017).

$$-CH_2-CF_2- + Li \rightarrow LiF + -CH = CF- + 0.5H_2 \quad (22)$$

The thermal runaway starts with the decomposition of solid-electrolyte-interface and involves the reaction of cathode, anode, and electrolyte. Several hydrocarbons are produced which brings potential of explosion and highly toxic fluorides such as HF and POF_3 are also formed which pose huge threat to safety.

Different equipment such as gas chromatography-mass spectrometry (GC–MS), gas chromatography/atomic emission detector (GC/AED), gas chromatography-flame ionization detector (GC-FID), nuclear magnetic resonance (NMR) spectroscopy, quadrupole mass spectrometry (QMS), quartz-enhanced photoacoustic spectroscopy (QEPAS), IC, and FTIR have been previously used to analyze the off-gas produced. It could be seen that by the outgassing of a LIB, a dangerous gas mixture with highly explosive, hazardous, and carcinogenic components is released. In general, the gas mixture would contain flammable components such as: H_2 and hydrocarbons; toxic components such as: fluoride, NO_x, SO_x, HCl, COS, acrolein; and components of both flammable and toxic: CO and electrolyte. Previous investigations of emission gases during handling of LIBs are summarized in Table 1.

3. Experimental

Four types of commercially available LIBs with geometrical format cylinder cell and pouch cell were investigated. Those cells used $LiCoO_2$ (LCO), $LiNi_xMn_yCo_zO_2$ (NMC), or $LiFePO_4$ (LFP) as cathode and carbon as anode. LCO 18650 and NMC 18650, rated to a nominal capacity of 3000 mAh and 2600 mAh respectively and are produced by Samsung. LFP 18650, rated to a nominal capacity of 1100mAh is produced by A123. LCO pouch cell, rated to a nominal capacity of 2500 mAh is produced by PKCELL. It is known from the cells' material safety data sheet that the electrolyte compositions are based on two or more mixtures of unknown weight ratios of diethyl carbonate (DEC), dimethyl carbonate (DMC), ethylene carbonate (EC), ethyl methyl carbonate (EMC), and propylene carbonate (PC). For all those cells, at least $LiFP_6$ are used as conducting salt.

The influence of different treatment methods, treating atmosphere and SOC were investigated. For LCO 18650 cells the complete SOC-window ranging from 0% to 100%, with intermediate steps of 50%, were investigated. For other types, a fully charged cell was used. Pyrolysis or combustion, and penetration tests were conducted to simulate thermal treatment and mechanical processing, respectively.

The thermal treatment was conducted in a programmable resistance furnace, as shown in Fig. 2. The reactor has a volume of 1 L and is sealed with a water cooling lid to create a fully closed environment. It contained a pressure gauge, a gas sampling vent, a thermocouple, a carrier gas inlet (Air/N_2) and an exhaust. Due to the small volume of the reactor, a special explosive container made of steel was designed to prevent distribution of particles in the sampling system and to protect the reactor during the heating process. Before starting the thermal treatment experiment, an explosive container charged with one battery was placed inside the reactor, steel chips were placed on the top of the container in the reactor as a dust filter. The exhaust was connected to the scrubber and a balloon was placed before the scrubber as a buffer during

Table 1
Summary of emission gases from LIBs.

Reference	Material		Test condition		Off-gas							Test equipment
	Cathode	Type	Method	Atm.	Electrolyte	CO_2	CO	H_2	C_xH_y	HF	Other	
Campion et al. (2004)			Heating			●				●	Fluoride	GC–MS, NMR
Ohsaki et al. (2005)	LCO	633,048	Overcharge			●	●	●	●			GC
Abraham et al. (2006)	NCA	18,650	Vent/ Penetration			●	●	●	●		C_2HF	GC–MS
Onuki et al. (2008)	NCA	Pouch	Heating	Ar		●	●	●	●			GC/AED
Ribière et al. (2012)	LMO	Pouch	Combustion test	Air		●	●		●	●	CO_2, HCN, NO_x, SO_x, HCl	FTIR, FID, paramagnetic analyzer
Wang et al. (2012)	LCO		TR			●		●	●	●	C_2H_5F	FTIR, GC–MS, NMR
Chanson (2013)	Li-ion		TR	Air		●	●	●	●	●		
Ponchaut et al. (2014)	LCO	Pouch	TR	Ar		●	●	●	●			GC–MS
Larsson et al. (2014b)	LFP	Pouch	Propane fire	Air		●				●	POF_3	FTIR
	LCO	633,048	Overcharge				●	●	●			GC
Golubkov et al. (2015)	NMC, LFP	18,650	Heating	Ar		●	●		●			GC
Lecocq et al. (2016)	LFP	Pouch	combustion	Air			●	●			SO_2	NDIR, FID, FTIR
Sun et al. (2016)	Li-ion	Both	Combustion	Air		●	●	●	●	●	SO_2, COS, $C_xH_yO_z$, $C_xH_yN_z$, C_5H_9NO	GC–MS, IC
Kwade et al. (2016)	NCM	Pouch	Penetration	N_2	●	●	●		●	●		FTIR
	NCM	18,650	Penetration	N_2	●	●	●		●	●		FTIR
	NCA	18,650	Penetration	N_2	●	●	●		●	●		FTIR
Nedjalkov et al. (2016)	NMC	Pouch	Penetration	Air	●	●	●		●	●	ClO_2, SO_2, Acrolein, COS	GC–MS, QMS, QEPAS, IC
Warner (2017)			Heating	Air		●			●	●	HCl, HCN,SO_2, H_2S	FTIR

"●": detected.

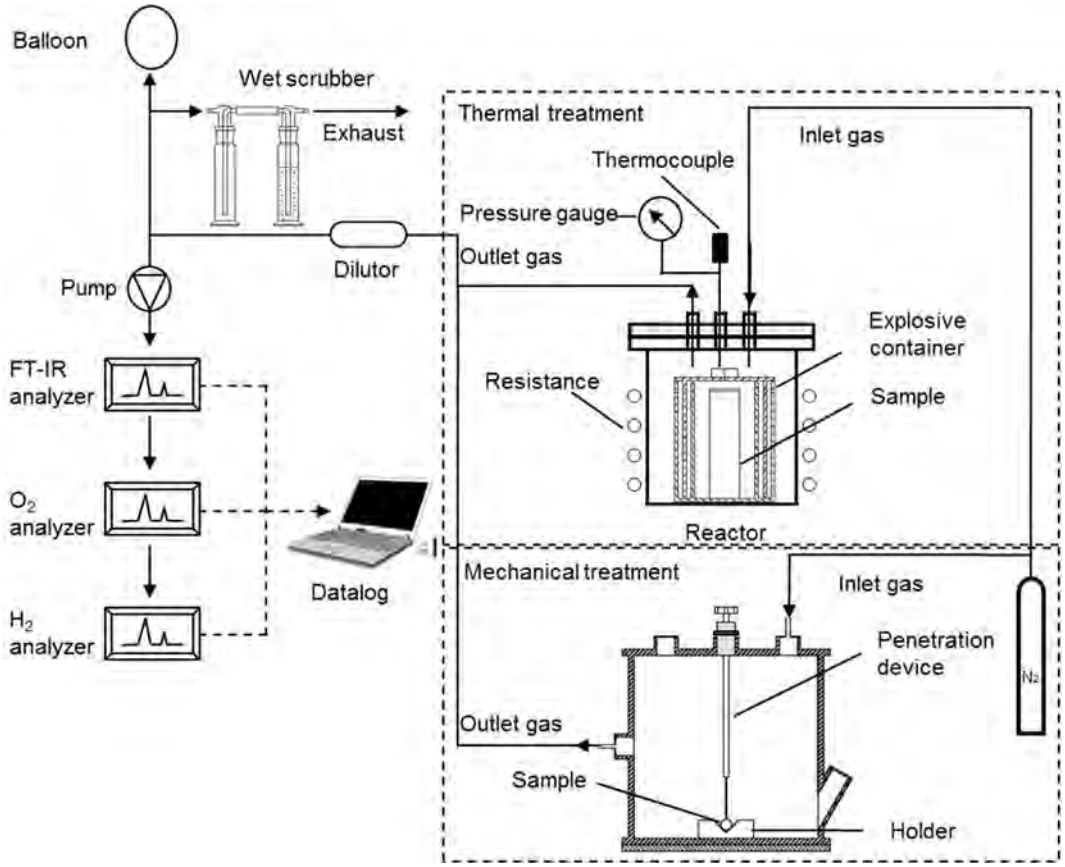

Fig. 2. Setup of quantitative thermal treatment off-gas analysis.

explosion. The function of the scrubber was to collect the halogen in off-gas. It contained two bottles, the first bottle was empty and acted as a safe buffer so as to prevent the liquid in the second bottle entering the reactor in case of pressure loss in the FTIR pump, whereas, the second bottle contained 200 mL 0.1 M NaOH to clean the off-gas. Gas sampling vent was connected to the sampling probe to collect samples of gas every 10 s during the process. N_2 was connected to the analyzers to be used as a carrier gas during the experiment. FTIR analyzer and O_2 analyzer were turned on and left in operation until their measuring cells reached the required temperature of 180 °C and 5 °C respectively. FTIR analyzer was calibrated manually using Calmet software. The main pump was adjusted to 1 L/min, whereas, the O_2 analyzer pump was adjusted to 0.4 L/min. Before the pyrolysis gas entered the FTIR, the gas was diluted with N_2 to a ratio of 1:14.

The penetration tests for quantitative analysis were carried out in a specially designed chamber equipped with a sealed penetration device, which have a triple nail in the form of trident at the penetration side. The cell was fixed in the groove of the holder and by pressing the penetration device, the penetration test was conducted. The nails (electric conductor steel) are supposed to simulate the shortcut between anodes to cathode due to the abuse of penetration. The FTIR was connected to the penetration reactor and similar process was conducted as indicated in Fig. 2. Additional IC tests were conducted after FTIR to analyze the concentrations of F and Cl caught in the washing bottles.

The FTIR analyzer used for these experiments corresponds to a Gasmet DX4000, which is a typical equipment used to measure H_2O, CO_2, CO, NO, NO_2, N_2O, SO_2, NH_3, CH_4, HCl, HF, and different volatile organic compounds. Samples of gases are collected using a portable sampling system, every 10 s and the sample cell is heated to 180 °C, to avoid any condensation of the produced gases. In addition to the Gasmet DX4000, PMA 10 paramagnetic O_2 Analyzer and LFE Conthos 3E thermal conductivity H_2 Analyzer were also employed to detect the concentration of O_2 and H_2 in vol %, respectively. The halogens samples were collected in washing bottles filled with 200 mL 0.1 M NaOH. Portion of the samples were transferred to the Ion chromatograph and inductively coupled plasma optical emission spectrometry (Metrogm Compact IC ion chromotograph).

4. Results and analysis

The amount of off-gas is calculated by integrating the time-concentration records from the FTIR, obtaining total volumes in NL, as shown in Eq. (23).

$$V = \frac{1}{\boldsymbol{d}} \sum_{i=0}^{n} \dot{\boldsymbol{V}}(t_{i+1} - t_i)(c_{i+1} + c_i)/2 \tag{23}$$

where V is the volume of compound (NL), d is the diluted ratio, $\dot{V}$ is flow rate of carried gas (NL/min), c_i is concentration of compound at time t_i (ppm), c_{i+1} is concentration of compound at time t_{i+1} (ppm).

The total volume of off-gas is obtained by summing the volume of all compounds together (refer to Fig. 3). The legends are displayed in order of battery type_ atmosphere_ SOC_ penetration or not. There are two penetration tests that underwent TR: fully charged LFP and pouch cell penetrated under N_2. Fig. 3 shows that LIBs produce the max amount of off-gas during combustion in air. Moreover, for the volume of off-gas produced in thermal treatment under air and N_2, it is clear that the amount of off-gas produced under air is more than that produced under N_2. The total amount of off-gas increases linearly with increasing mass loss, except for the off-gas produced during combustion in air. This observation can be explained since in thermal treatment of LIB under N_2 (Pyrolysis) decompose the organics and produces in addition to the gas products a solid char (coke) that remains in the material. This means that not all organic material can fully be removed from the batteries. In contrast, during combustion, the available oxygen react with organics promoting combustion reactions (CO_2, CO, H_2O) that leads to fully gasification of organics from the target material. It is also important to mention that comparing off-gas production and mass loss between battery cell types can be challenging as different cells have different geometries and amount of electrolytes/organics. Therefore, LCO can be considered the center or model of the whole study since all parameters were evaluated for this battery. Other battery cells can only be taken as indicators. Comparing the volume of off-gas produced in penetration test and that produced in thermal treatment, it can be seen that thermal treatment produces more off-gas than penetration test. Penetration test produces the minimum amount of off-gas and has the lowest mass loss. This can be easily explained as the main reaction happening was the boiling of electrolyte solvents after opening the batteries as detected with the FTIR. However, when TR occurs during penetration test both the amount of off-gas and the mass loss increase greatly compared to that without TR.

In Fig. 4, an example (LCO pouch cell) of the material before and after penetration test and pyrolysis trial is shown. As it is noticed, major damage occurred during thermal treatment (pyrolysis) and penetrations test with an SOC of 100%. The main reason for this similarity is the TR reactions that takes place in both conditions reached temperatures higher than 700 °C, as evidenced by partial melting of aluminum foils. The Penetration test with 50% SOC did not experience TR during treatment. Therefore, weight loss is very low compared to other conditions, as indicated in Fig. 3.

4.1. Evaluation of toxicity

Although growing attention has been paid to investigate the off-gas produced by LIBs, so far no method is put forward to carry out a quantitative evaluation of toxicity of total off-gas produced by LIBs. In addition, considering the complex issue of fire toxicity (Stec and Hull, 2010), the toxicity of LIBs in case of TR is even more complex due to the specific chemistry of their components compared to conventional fuels (Lecocq et al., 2016). In this case, a new method is proposed to give an evaluation of toxicity of the total off-gas produced by LIBs.

USA's Protective Action Criteria (PAC) is introduced here to undertake a quantitative comparison of toxicity of total off-gas. PAC_1, which is the mildest toxic concentration of substance, is used to perform the following calculations (ATL International, 2012; Hess et al., 2014).

Namely, theoretical contaminated volume of single LIB is calculated to evaluate the toxicity. Assuming that there is no condensation during the detection period and interaction among different compounds can be negligible, the theoretical contaminated volume of single LIB can be expressed as the sum of the volumes required to guarantee the human health for all the substances detected in off-gas:

$$V_c\text{ontaminated} = \sum \frac{V\_substance}{PAC\_1} \tag{24}$$

The higher the theoretical contaminated volume is, the more toxic the off-gas becomes. Fig. 5 depicts PAC_1 theoretical contaminated volume for a single fully charged cell. Here the four axes are on behalf of four types of cells: LCO 18650, NMC 18650, LFP 18650, and LCO pouch cell. The values on the axis stand for theoretical contaminated volume pre cell in unit of m^3. TR occurs when penetrating fully charged LFP 18650 and LCO pouch cell under N_2.

As indicated in Fig. 5, pyrolyzed LFP 18650 cell under N_2 produces the most acute off-gas with a theoretical contaminated volume of 379 m^3 while combusted LCO pouch cell under air produces

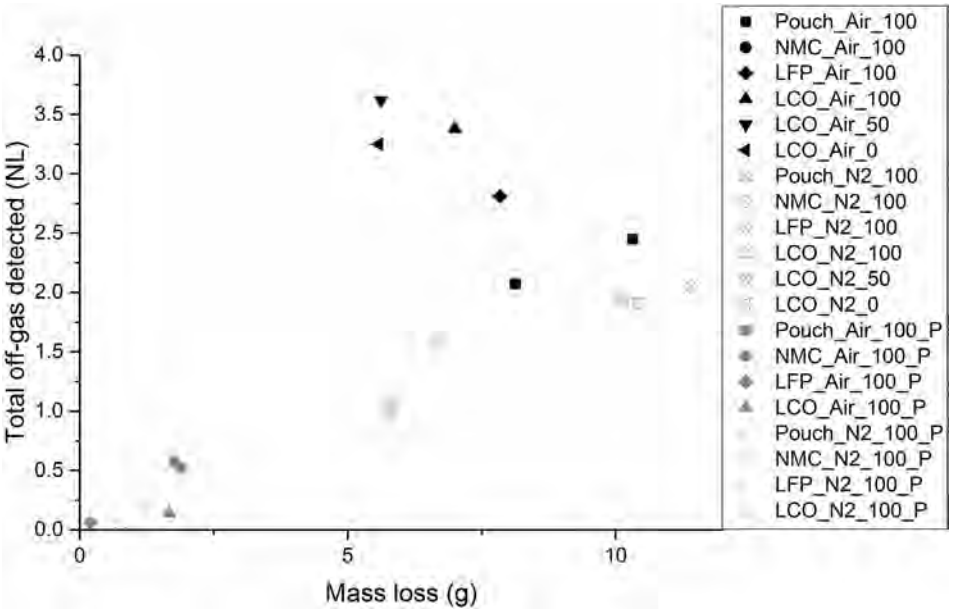

Fig. 3. Mass loss vs. total off-gas volume detected per single Li-ion battery cell.

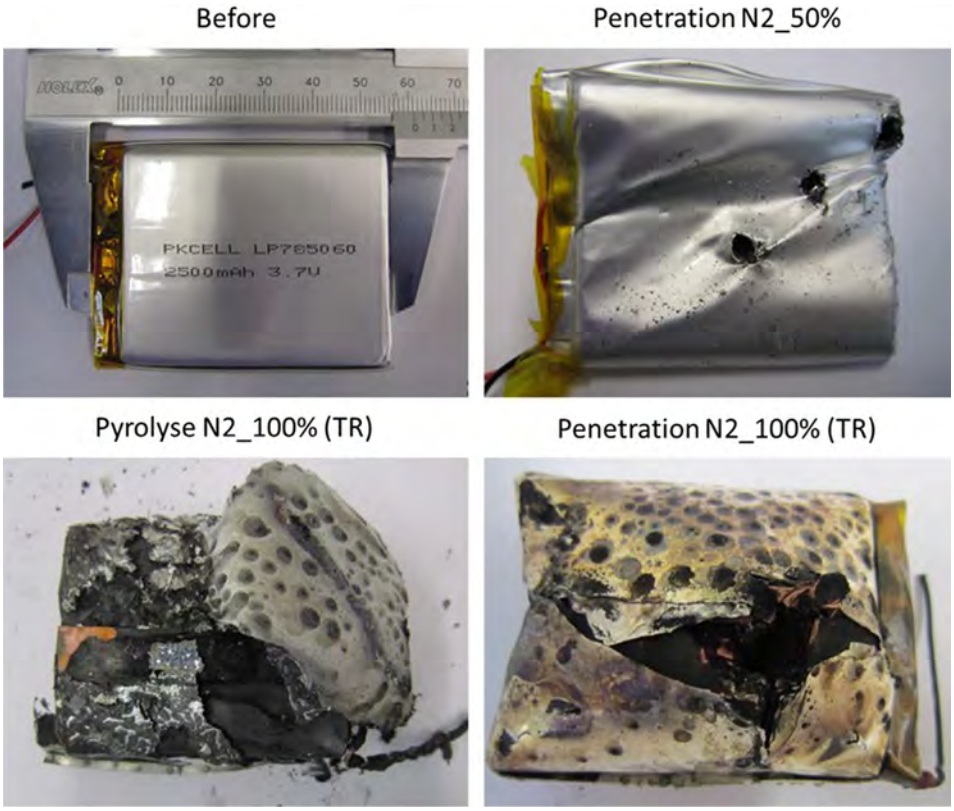

Fig. 4. Li-ion pouch cell (pouch) before and after penetration and pyrolysis test.

the less hazardous off-gas in thermal treatment with a theoretical contaminated volume of 72 m^3. Thermal treatment produces more toxic off-gas than mechanical treatment. The toxicity of off-gas produced during pyrolysis under N_2 is higher than that produced during combustion under air for fully charged NMC, LFP and pouch cells.

As indicated in Fig. 6, at least ten species of toxic gases were detected (DC, EC, PC, DMC, HCl, CO, Acrolein, COF_2; HF and Formadehyde). Their presence can be explained with the literature but their exact pathway can be rather complex and difficult to fully understand. Nevertheless, it was already reported in previous work that during thermal treatment (Diaz et al., 2018), the first phenomena correspond to simple dehydration reactions of water and electrolyte that occurs between 100 and 250 °C. This can explain the presence of H_2O and some electrolyte solvents like EC, PC and DMC as described in reactions (3)–(5). After that, degradation of

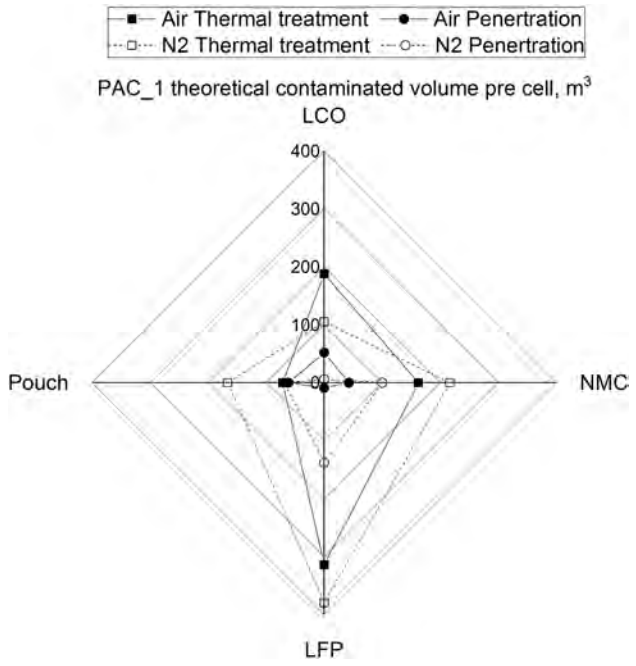

Fig. 5. PAC_1 contaminated volume of four types of fully charged single cells.

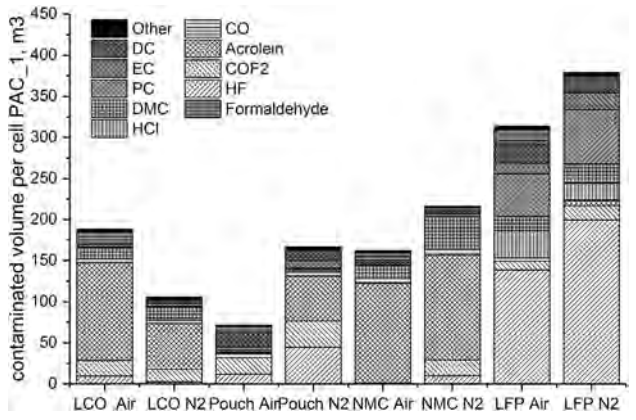

Fig. 6. Theoretical contaminated volumes for individual substances of four types of fully charged cells after thermal treatments (pyrolysis and combustion).

the electrolyte and solvents takes place together with degradation of SEI leading to formation of hydrocarbons (C_xH_y) and CO_2. The last one as a result of combustion reactions with the most probably oxygen source in the form of hydroxyl radicals produced during degradation of organics. Some oxidation reactions are described in equations (11)–(13). Like this, CO can be also formed as incomplete combustion of hydrocarbons. It could also be observed that by increasing the temperature formation of HF and other fluorides like POF_3, PF_4OH, C_2H_5F is expected as registered in reactions (14)–(21). All detected toxic gases contribute to the theoretical contaminated volume and their share in the total volume can be observed in Fig. 6.

It can be seen from Fig. 6 that the theoretical contaminated volumes caused by HF, COF_2, acrolein, CO, HCl, formaldehyde, and electrolyte solvent (PC, EC, DEC, and DMC) account for more than 96% of the total theoretical contaminated volume. This suggests that HF, COF_2, acrolein, CO, HCl, formaldehyde, and electrolyte solvent are the most important toxic compounds for evaluating the toxicity of off-gas produced by LIB. The work published by Nedjalkov et al. (Nedjalkov et al., 2016) in 2016 indicated a similar result that electrolyte solvent, benzene, toluene, styrene, biphenyl, acrolein, CO, COS, and HF were the eleven crucial gas mixture constituents for damaged LIB. This is also consistent with the study of Ribière et al. (2012) who investigated the fire-induced hazards of LIBs. They identified the toxic emissions of HF, CO, NO, SO_2, and HCl as the first order evaluation of the danger of toxic gases. Larsson and Andersson et al. (Andersson et al., 2016; Larsson et al., 2017, 2014a, 2014b) have also investigated toxic gas emissions from LIB fires. Their studies focused on the quantitative analysis of emission of the fluorides.

The influence of SOC on theoretical contaminated volume is shown in Fig. 7. No obvious tendency is observed for the total theoretical contaminated volume with increasing SOC. The theoretical contaminated volume of cell with 50% SOC is higher than that with 0% and 100% SOC during combustion under air while that is lower during pyrolysis under N_2.

It could be also seen from Fig. 7 that the contaminated volumes of fluorides decrease with increasing SOC. This is in accordance to the study of Larsson et al. (2017), that the total amount of HF was higher at decreasing the SOC. Similar, Ribière et al. (2012) have found out that only HF concentration in the off gas indicated a SOC dependence. For this particular case, the maximum concentration was achieved with fully discharged batteries. Lecocq et al. (2016) have also detected the same tendency.

Although the amount of HF decreases with increasing SOC, other fluorides have a different tendency, as depicted in Fig. 8. The mole amount of substance (mol) is calculated by using perfect gas law:

$$n = V/22.4(NL/mol) * i \quad (25)$$

where n is the mole amount of substance (mol), i is the number of specific atoms contented in compound formula.

Considering the two most detected fluorides HF and CF_4, it could be observed that their formation is highly affected by the state of charge of the battery, as stability of one or the other variates with this as well as with the type of atmosphere (Air or N_2). In Fig. 8, the molar amount of fluorine in the total volume of each specie was calculated and plotted in a single figure. By contrasting the F emitted as HF and CF_4, it is possible to predict their distribution in the gas produced during the thermal treatment. As it can be seen the mole amount of F emitted as HF increases with the mole amount of F emitted as CF_4 decreasing: at 100% SOC, the mole amount of F in HF is the lowest and the mole amount of F in CF_4 is the highest, while at 0% SOC the opposite results are obtained. It seems that HF is more likely to be formed in case of thermally treated low SOC cells. This could be explained by the preliminary theory of Scheirs et al.'s (Scheirs and Kaminsky, 2006) that higher

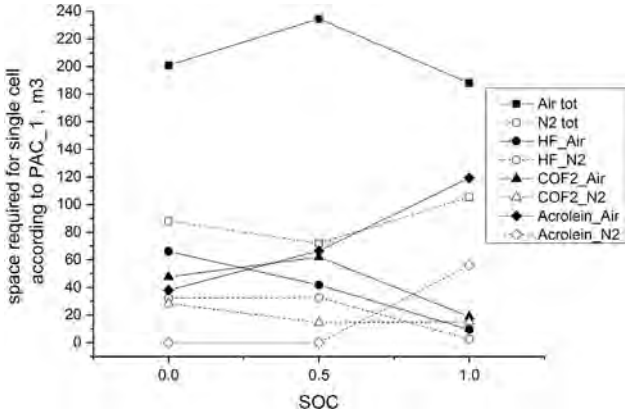

Fig. 7. Space required to thermally treat (pyrolysis and combustion) a LCO cylinder cell based on the theoretical contaminated volume PAC_1 vs SOC.

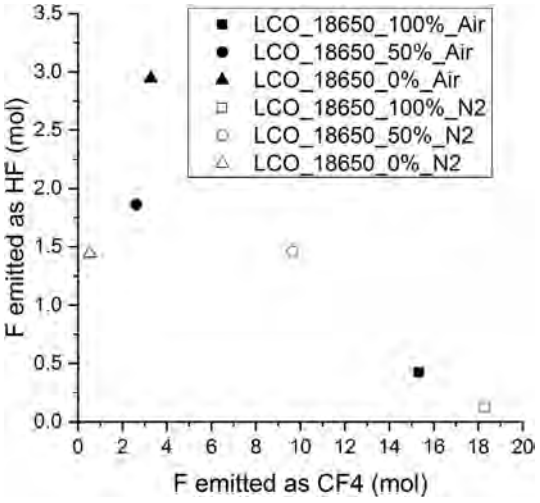

Fig. 8. Relation between amount of fluor in moles emitted as HF or CF_4 under different scenarios in SOC and atmosphere.

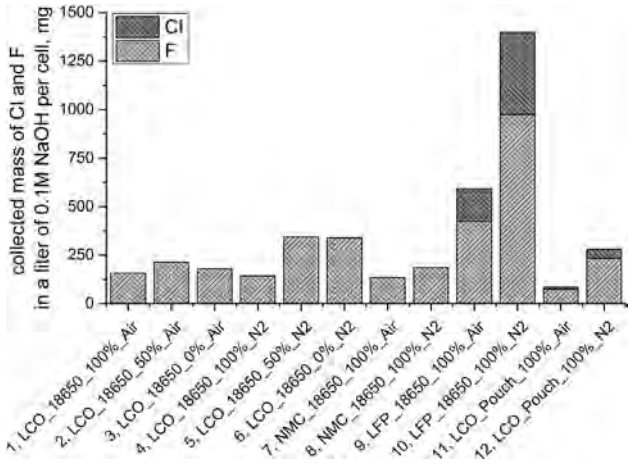

Fig. 9. Analysis of halides collected in the scrubber (0.1 M NaOH) after thermal treatment of four different types of Li-ion batteries and atmospheres (N2 and Air).

temperature and higher heating rate intensified the bond breaking and production of small molecules. Although production of HF can be easily explained with the reported data, mechanism of formation of CF_4 from LIBs could not be completely understood in the present study. However, most probably during heating the fully charged cell, TR takes place and temperature and heating rate increase drastically leading to formation of small molecules of difficult formation such as pure H_2 and CF_4.

Emissions of CO, HF and POF_3 were found in TR reactions in accordance to a recent work published by Larsson et al. (2018). Toxicity of CO and HF has been documented in the past. However, toxicity of POF_3 is strongly related to possible formation of HF, as this compound is considered as precursor by hydrolysis (see Eqs. (14), (26) and (27)), (Larsson et al., 2018), where water/humidity is enough to produce HF, thus, its relevance.

$$PF_5 + H_2O \rightleftharpoons POF_3 + 2HF \quad (26)$$

$$POF_3 + 3H_2O \rightleftharpoons H_3PO_4 + 3HF \quad (27)$$

4.2. Verification of halogens detected in FTIR

The presence of fluorine can be easily understood due to the Fl-containing electrolyte and the PVDF binder in the LFP batteries (Feng et al., 2017; Ortner and Hensler, 1995). As well, chlorine can be found as inorganic electrolyte in the form of e.g. $LiClO_4$ (Julien et al., 2015; Marom et al., 2010) or also in the plastic covers as flame retardants. Due to the high toxicity and relative large emission volume of halogens compared to other crucial toxic compounds for LIB off-gas, additional IC tests are conducted again after FTIR to analyze the total F^- and Cl^- trapped in $NaOH_{aq}$. The analysis is carried for thermal treatments and some for the penetration tests. Concentrations lower than 10 mg/L are neglected.

As it is shown in Fig. 9, LFP 18650 cells produce the maximum amount of fluorides and chlorides both under air and N_2 among the four types of LIBs used for this work. By comparison of No. 1–3 and 4–6, it can be noticed that discharged cells show the highest fluorides values. This consists with the volume of HF calculated in FTIR detection. In addition, by comparing No. 7 and 8, 9 and 10, and 11 and 12, it can be concluded that the amount of soluble halides (in NaOH) produced by thermal treatment under N_2 is higher than that produced under air. At this point, the lack of halides removed in the scrubber during combustion with air, indicates the possibility of formation of unknown halides that are hardly soluble in NaOH, or formation of dioxins/furans which might be distributed in the gas outlet of the reactor, piping or first empty bottle. The last one, can be possible as formation of such a compounds can be supported by the presence of oxygen, which leads to the halogen elimination in the HCL or HF followed by hydroxyl radical addition. The addition reactions of OH leads to formation of PCDD/F products (Environment Australia, 1999). This is also supported by Lopes et al. (2015), where authors recommended to undergo the gasification of combustion of waste under oxygen deficit to avoid formation of dioxins and furans.

5. Conclusions

It is observed that compared to thermal treatment, penetration test produces less amount and less toxic off-gas. For thermal treatment, SOC has no obvious influence on the toxicity of total off-gas produced for LCO Cells. However, the type of gas varies with the SOC. For instance, HF is reported to be more stable at low SOC (0%) than that at high SOC (100%), leading to the formation of other undetected fluorides like CF_4. This observation fitted with previous published work (Ribière et al., 2012; Lecocq et al., 2016). However, Due to the non-conclusive results in terms of theoretical contaminated volume by variating the SOC for LCO cells further studies with other cell types should be conducted to get a more certain picture for this parameter.

In general, combustion produces more off-gas at the same time that the toxicity of off-gas is reduced compared to pyrolysis in N_2. Among the four types of cells used in this work, LFP generates the most dangerous off-gas during thermal treatment. HF, COF_2, acrolein, CO, formaldehyde, HCl, and electrolyte solvents are the most toxic compounds, they account for more than 96% of the total theoretical contaminated volumes.

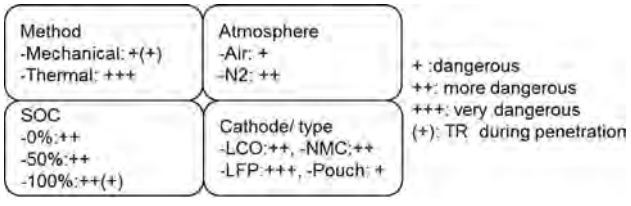

Fig. 10. Summarized assessments on the Influence of different factors on toxicity in the off-gas produced by LIBs recycling.

From the main findings, the following can be highlighted:

1. Compared with thermal treatment, penetration test without TR produces less amount (less than 20% of the off-gas produced during combustion) and less toxic off-gas. When there is no TR taking place during penetration test, the emission of off-gas is relative mild, this means that most of the electrolytes will go with the material to next mechanical processing steps. Also, it is no possible to control the emission of the electrolytes.
2. For NMC, LFP, and pouch cell, although combustion produces 1–2 times more off-gas than pyrolysis under N_2, the theoretical contaminated volume of off-gas is reduced by more than 50 m^3.
3. A new method is proposed to perform an evaluation of the toxicity of total off-gas. HF, COF_2, acrolein, CO, formaldehyde, HCl, and electrolyte solvents are the most important toxic compounds we need to consider in recycling processes by taking both of the toxicity and emission amount into consideration. They account for more than 96% of the total theoretical contaminated volumes.
4. Influence of type and amount of electrolyte should be considered. The influence of cathode material is studied in this work. However, the electrolytes used for those cells might also be different. The types and volumes of the electrolyte solvents and conducting salts have great influence on the off-gas, for example: off-gas produced by LFP and LCO pouch cells includes chloride which is likely to be caused by the special conducting salts they use. So the influence of electrolyte cannot be neglected.
5. Different types of LIBs have different kinds of behaviors during recycling. Among the four types of cells used in this work, LFP generates the most dangerous off-gas during thermal treatment. For one single LFP cell, space of 379 m^3 is required to ensure a safety environment for human health. So far LFP is regarded as the safest LIB due to its superior thermal stability. However, when it comes to recycling, the toxicity of the off-gas it produced is 2 times higher than other types of LIBs.
6. The off-gases generated during thermal treatment and mechanical processing of LIBs are of acute toxicity. Great attention should be paid and safety handling must be carried out for the off-gas of LIBs. The Influence of different factors to toxicity of off-gas produced by recycling LIBs is demonstrated in Fig. 10. Mechanical treatment of discharged cells under air is suggested as pretreatment process in term of minimization of toxic gases.

References

Abraham, D.P., Roth, E.P., Kostecki, R., McCarthy, K., MacLaren, S., Doughty, D.H., 2006. Diagnostic examination of thermally abused high-power lithium-ion cells. J. Power Sources 161 (1), 648–657. https://doi.org/10.1016/j.jpowsour.2006.04.088.

Amarakoon, S., Smith, J., Segal, B., 2013. Application of Life-Cycle Assessment to Nanoscale Technology: Lithium-ion Batteries for Electric Vehicles EPA 744-R-12-001, 126 pp. https://www.epa.gov/sites/production/files/2014-01/documents/lithium_batteries_lca.pdf. Accessed 25 May 2018.

Andersson, P., Blomqvist, P., Lorén, A., Larsson, F., 2016. Using Fourier transform infrared spectroscopy to determine toxic gases in fires with lithium-ion batteries. Fire Mater. 40 (8), 999–1015. https://doi.org/10.1002/fam.2359.

ATL International, I., 2012. Table 2: Protective Action Criteria (PAC) Rev. 29 based on applicable 60-minute AEGLs, ERPGs, or TEELs. https://sp.eota.energy.gov/pac/docs/Revision_29_Table2.pdf. Accessed 25 May 2018.

Bloom, I., Cole, B.W., Sohn, J.J., Jones, S.A., Polzin, E.G., Battaglia, V.S., Henriksen, G.L., Motloch, C., Richardson, R., Unkelhaeuser, T., Ingersoll, D., Case, H.L., 2001. An accelerated calendar and cycle life study of Li-ion cells. J. Power Sources 101 (2), 238–247. https://doi.org/10.1016/S0378-7753(01)00783-2.

Campion, C.L., Li, W., Euler, W.B., Lucht, B.L., Ravdel, B., DiCarlo, J.F., Gitzendanner, R., Abraham, K.M., 2004. Suppression of toxic compounds produced in the decomposition of lithium-ion battery electrolytes. Electrochem. Solid-State Lett. 7 (7), A194. https://doi.org/10.1149/1.1738551.

Chanson, C., 2013. Li-ion batteries safety. agoria 25, pp.

Chen, Y., Tang, Z., Lu, X., Tan, C., 2006. Research of explosion mechanism of lithium-ion battery. Prog. Chem. 18 (06), 823–831.

Diaz, F., Wang, Y., Moorthy, T., Friedrich, B., 2018. Degradation Mechanism of Nickel-Cobalt-Aluminum (NCA) cathode material from spent lithium-ion batteries in microwave-assisted pyrolysis. Metals 2018 (8), 565. https://doi.org/10.3390/met8080565.

Doerffel, D., Sharkh, S.A., 2006. A critical review of using the Peukert equation for determining the remaining capacity of lead-acid and lithium-ion batteries. J. Power Sources 155 (2), 395–400. https://doi.org/10.1016/j.jpowsour.2005.04.030.

European Li-Ion Battery Advanced Manufacturing for Electric Vehicles (ELIBAMA), 2014. Li-ion BATTERIES RECYCLING. The batteries end of life..., Available online: http://www.webcitation.org/717f6wRdJ. Accessed on 14 August 2018.

Environment Australia, 1999. Incineration and Dioxins: Review of Formation Processes, consultancy report prepared by Environmental and Safety Services for Environment Australia, Commonwealth Department of the Environment and Heritage, Canberra.

Feng, X., Ouyang, M., Liu, X., Lu, L., Xia, Y., He, X., 2017. Thermal runaway mechanism of lithium ion battery for electric vehicles: A review. Energy Storage Mater. https://doi.org/10.1016/j.ensm.2017.05.013.

Georgi-Maschler, T., Friedrich, B., Weyhe, R., Heegn, H., Rutz, M., 2012. Development of a recycling process for Li-ion batteries. J. Power Sources 207, 173–182. https://doi.org/10.1016/j.jpowsour.2012.01.152.

Golubkov, A.W., Scheikl, S., Planteu, R., Voitic, G., Wiltsche, H., Stangl, C., Fauler, G., Thaler, A., Hacker, V., 2015. Thermal runaway of commercial 18650 Li-ion batteries with LFP and NCA cathodes – impact of state of charge and overcharge. RSC Adv. 5 (70), 57171–57186. https://doi.org/10.1039/C5RA05897J.

Hess, S., Wohlfahrt-Mehrens, M., Wachtler, M., 2014. Flammability of li-ion battery electrolytes: flash point and self-extinguishing time measurements. J. Electrochem. Soc. 162 (2), A3084–A3097. https://doi.org/10.1149/2.0121502jes.

Ortner, J., Hensler, G., 1995. Beurteilung von Kunststoffbränden: bei einer Störung des bestimmungsgemäßen Betriebs entstehende Stoffe nach den Anhängen II - IV der 12. BImSchV. https://www.lfu.bayern.de/luft/doc/kunststoffbraende.pdf. Accessed 26 May 2018.

Julien, C., Mauger, A., Vijh, A., Zaghib, K., 2015. Lithium Batteries Science and Technology. Springer, Cham, pp. 29–68. 1007/978-3-319-19108-9.

Kawamura, T., Kimura, A., Egashira, M., Okada, S., Yamaki, J.-I., 2002. Thermal stability of alkyl carbonate mixed-solvent electrolytes for lithium ion cells. J. Power Sources 104 (2), 260–264. https://doi.org/10.1016/S0378-7753(01)00960-0.

Kwade, A., Diekmann, J., Hanisch, C., Spengler, T., Thies, C., Dröder, K., Cerdas, J., Gerbers, R., Herrmann, C., Scholl, S., Stehmann, F., Haas, P., Kurrat, M., Hauck, D., 2016. Recycling von Lithium-Ionen-Batterien – LithoRec II. Institut für Partikeltechnik, Institut für Automobilwirtschaft und Industrielle Produktion, Institut für Werkzeugmaschinen und Fertigungstechnik, Institut für Chemische und Thermische Verfahrenstechnik, Institut für Hochspannungstechnik und elektrische. Energieanlagen 239, pp.

Larsson, F., Andersson, P., Mellander, B., 2014a. Battery Aspects on Fires in Electrified Vehicles. Third International Conference on Fires in Vehicles. October 1st-2nd. Berlin, Germany, p. 209.

Larsson, F., Andersson, P., Blomqvist, P., Lorén, A., Mellander, B.-E., 2014b. Characteristics of lithium-ion batteries during fire tests. J. Power Sources 271, 414–420. https://doi.org/10.1016/j.jpowsour.2014.08.027.

Larsson, F., Andersson, P., Blomqvist, P., Mellander, B.-E., 2017. Toxic fluoride gas emissions from lithium-ion battery fires. Sci. Rep. 7 (1), 10018. https://doi.org/10.1038/s41598-017-09784-z.

Larsson, F., Bertilsson, S., Furlani, M., Albinsson, E., Mellander, B., 2018. Gas explosions and thermal runaways during external heating abuse of commercial lithium-ion graphite-LiCoO2 cells at different levels of ageing. J. Power Sources 373, 220–231. https://doi.org/10.1016/j.jpowsour.2017.10.085.

Lecocq, A., Eshetu, G.G., Grugeon, S., Martin, N., Laruelle, S., Marlair, G., 2016. Scenario-based prediction of Li-ion batteries fire-induced toxicity. J. Power Sources 316, 197–206. https://doi.org/10.1016/j.jpowsour.2016.02.090.

Li, L., Lu, J., Ren, Y., Zhang, X.X., Chen, R.J., Wu, F., Amine, K., 2012. Ascorbic-acid-assisted recovery of cobalt and lithium from spent Li-ion batteries. J. Power Sources 218, 21–27. https://doi.org/10.1016/j.jpowsour.2012.06.068.

Li, L., Chen, R., Sun, F., Wu, F., Liu, J., 2011. Preparation of LiCoO2 films from spent lithium-ion batteries by a combined recycling process. Hydrometallurgy 108, 220–225. https://doi.org/10.1016/j.hydromet.2011.04.013.

Linden, D., Reddy, T.B., 2002. In: Handbook of batteries. 3rd ed. McGraw-Hill, New York, NY, p. 0071359788.

Lopes, E.J., Okamura, L.A., Yamamoto, C.I., 2015. Formation of dioxins and furans during municipal solid waste gasification. Braz. J. Chem. Eng. 32 (1), 87–97. https://doi.org/10.1590/01046632.20150321s00003163.

Marom, R., Halk, O., Aurbach, D., Halalay, I., 2010. Revisiting LiClO4 as an electrolyte for rechargeable lithium-ion batteries. J. Electrochem. Soc. 157 (8), A972–A983. https://doi.org/10.1149/1.3447750.

Nedjalkov, A., Meyer, J., Köhring, M., Doering, A., Angelmahr, M., Dahle, S., Sander, A., Fischer, A., Schade, W., 2016. Toxic gas emissions from damaged lithium ion batteries—analysis and safety enhancement solution. Batteries 2 (1), 5. https://doi.org/10.3390/batteries2010005.

Ohsaki, T., Kishi, T., Kuboki, T., Takami, N., Shimura, N., Sato, Y., Sekino, M., Satoh, A., 2005. Overcharge reaction of lithium-ion batteries. J. Power Sources 146 (1–2), 97–100. https://doi.org/10.1016/j.jpowsour.2005.03.105.

Onuki, M., Kinoshita, S., Sakata, Y., Yanagidate, M., Otake, Y., Ue, M., Deguchi, M., 2008. Identification of the source of evolved gas in li-ion batteries using [sup 13] C-labeled solvents. J. Electrochem. Soc. 155 (11), A794. https://doi.org/10.1149/1.2969947.

Pillot, C., 2013. Micro hybrid, HEV, P-HEV and EV market 2012–2025 impact on the battery business. In: Electric Vehicle Symposium and Exhibition (EVS27). 17–20 Nov. 2013. Barcelona, Spain, p. 6.

Pillot, C., 2017a. The rechargeable battery market 2016-2025. 20th March. 2019. Fort Lauderdale, FL, USA.

Pillot, C., 2017b. Lithium ion battery raw material supply & demand 2016-2025. Advanced Automotive Battery Conference. 01.30.17. Maiz, Germany, 42 pp.

Ponchaut, N., Marr, K., Colella, F., Somandepalli, V., Horn, Q., 2014. Thermal Runaway and Safety of Large Lithium-Ion Battery Systems. Exponent Inc., Natick, MA, p. 01760.

Ribière, P., Grugeon, S., Morcrette, M., Boyanov, S., Laruelle, S., Marlair, G., 2012. Investigation on the fire-induced hazards of Li-ion battery cells by fire calorimetry. Energy Environ. Sci. 5 (1), 5271–5280. https://doi.org/10.1039/C1EE02218K.

Röder, P., Baba, N., Friedrich, K.A., Wiemhöfer, H.-D., 2013. Impact of delithiated Li0FePO4 on the decomposition of LiPF6-based electrolyte studied by accelerating rate calorimetry. J. Power Sources 236, 151–157. https://doi.org/10.1016/j.jpowsour.2013.02.044.

Scheirs, J., Kaminsky, W., 2006. Feedstock recycling and pyrolysis of waste plastics: Converting waste plastics into diesel and other fuels. J. Wiley & Sons, Chichester UK, Hoboken NJ, p. 785. xxvii 9780470021521.

Spotnitz, R., Franklin, J., 2003. Abuse behavior of high-power, lithium-ion cells. J. Power Sources 113 (1), 81–100. https://doi.org/10.1016/S0378-7753(02)00488-3.

Stec, A.A., Hull, T.R., 2010. Fire Toxicity. Elsevier, p. 184569807X.

Sun, J., Li, J., Zhou, T., Yang, K., Wei, S., Tang, N., Dang, N., Li, H., Qiu, X., Chen, L., 2016. Toxicity, a serious concern of thermal runaway from commercial Li-ion battery. Nano Energy 27, 313–319. https://doi.org/10.1016/j.nanoen.2016.06.031.

Sun, L., Qiu, K., 2011. Vacuum pyrolysis and hydrometallurgical process for the recovery of valuable metals from spent lithium-ion batteries. J. Hazard. Mater. 194, 378–384. https://doi.org/10.1016/j.jhazmat.2011.07.114.

Tobishima, S.-I., Yamaki, J.-I., 1999. A consideration of lithium cell safety. J. Power Sources 81–82, 882–886. https://doi.org/10.1016/S0378-7753(98)00240-7.

U.S. environmental protection agency, 2011. Electronics waste management in the United States through 2009, 49 pp.

Wang, H., Friedrich, B., 2015. Development of a highly efficient hydrometallurgical recycling process for automotive li–ion batteries. J. Sustain. Metall. 1 (2), 168–178. https://doi.org/10.1007/s40831-015-0016-6.

Wang, Q., Ping, P., Zhao, X., Chu, G., Sun, J., Chen, C., 2012. Thermal runaway caused fire and explosion of lithium ion battery. J. Power Sources 208, 210–224. https://doi.org/10.1016/j.jpowsour.2012.02.038.

Warner, N., 2017. Overview of a year of battery fire overview of a year of battery fire testing by DNV GL for Con Ed, NYSERDA and FDNY 34. DNV GL, NFPA 855 Committee Meeting. https://nysolarmap.com/media/1743/n-warner_dnv-gl-battery-testing-results.pdf. Accessed 26 May 2018.

Zeng, X., Li, J., Singh, N., 2014. Recycling of spent lithium-ion battery: a critical review. Crit. Rev. Environ. Sci. Technol. 44 (10), 1129–1165. https://doi.org/10.1080/10643389.2013.763578.